LUNAR FORMATION

Oxygen isotopic evidence for vigorous mixing during the Moon-forming giant impact

Edward D. Young,[1]* Issaku E. Kohl,[1]* Paul H. Warren,[1] David C. Rubie,[2] Seth A. Jacobson,[2,3] Alessandro Morbidelli[3]

Earth and the Moon are shown here to have indistinguishable oxygen isotope ratios, with a difference in $\Delta'^{17}O$ of −1 ± 5 parts per million (2 standard error). On the basis of these data and our new planet formation simulations that include a realistic model for primordial oxygen isotopic reservoirs, our results favor vigorous mixing during the giant impact and therefore a high-energy, high-angular-momentum impact. The results indicate that the late veneer impactors had an average $\Delta'^{17}O$ within approximately 1 per mil of the terrestrial value, limiting possible sources for this late addition of mass to the Earth-Moon system.

The Moon is thought to be the consequence of a giant collision between the proto-Earth and a planetary embryo (named Theia, "mother of the Moon") ~10^8 years after the birth of the solar system (*1*, *2*). However, the distinct oxygen isotopic signatures of solar system bodies (*3*, *4*) has presented a problem for the impact hypothesis for the formation of the Moon (*5*, *6*). In order to create an iron-poor Moon and simultaneously reproduce the angular momentum of the Earth-Moon system, early models required a glancing blow by a Mars-sized impactor that resulted in the Moon being composed mainly of impactor material (*7*). Therefore, in the general case the Moon and Earth should not be identical in their oxygen isotopic compositions. Nonetheless, until recently the Moon and Earth have been found to be indistinguishable in their oxygen isotope ratios (*8*–*10*). Proposed higher-energy giant impacts offer potential solutions to this conundrum (*11*), although at the expense of the need to shed substantial angular momentum from the system via orbital resonances (*12*).

Oxygen reservoirs comprising rocky bodies of the solar system are characterized by distinct relative concentrations of oxygen isotopes. These relative concentrations are customarily represented by $\Delta^{17}O$, the departure in $^{17}O/^{16}O$ relative to a given $^{18}O/^{16}O$ under the assumption that these two isotope ratios covary as a consequence

[1]Department of Earth, Planetary, and Space Sciences, University of California Los Angeles, Los Angeles, CA, USA. [2]Bayerisches Geoinstitut, University of Bayreuth, D-95490 Bayreuth, Germany. [3]Laboratoire Lagrange, Université de Nice–Sophia Antipolis, Observatoire de la Cote d'Azur, CNRS, 06304 Nice, France.
*Corresponding author E-mail: eyoung@epss.ucla.edu (E.D.Y.); ikohl@epss.ucla.edu (I.E.K.)

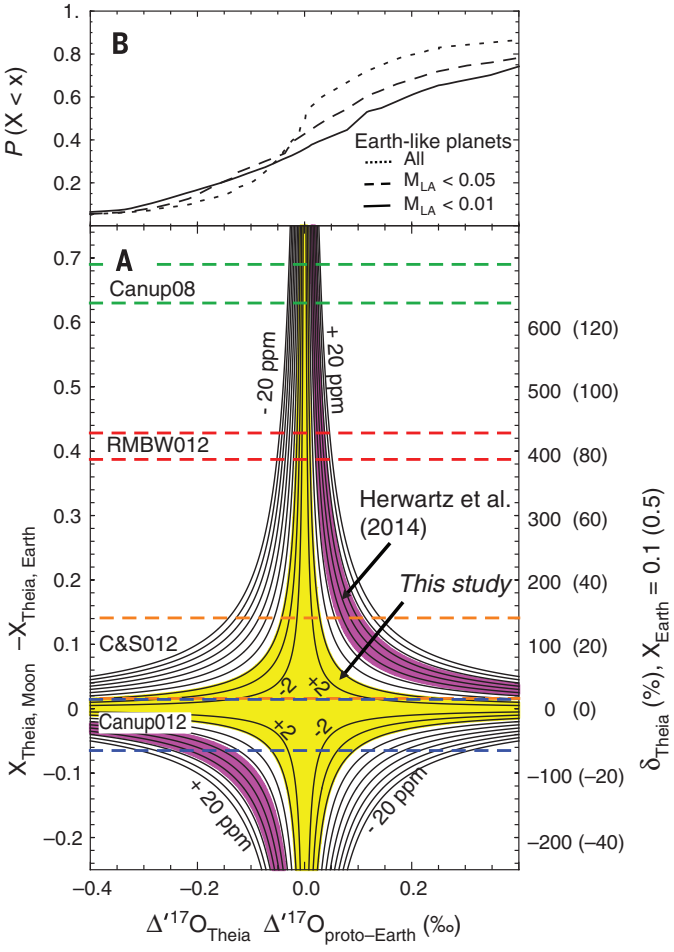

Fig. 1. Oxygen isotope mass balance diagram. (**A**) Contours of $\Delta'^{17}O_{Moon} - \Delta'^{17}O_{Earth}$ in parts per milliion versus fractional differences in Theia content of the bulk silicate Moon and Earth and $\Delta'^{17}O_{Theia} - \Delta'^{17}O_{proto\text{-}Earth}$. The contour interval is 2 ppm. The pink region indicates that the contour intervals are consistent with the $\Delta'^{17}O_{Moon} - \Delta'^{17}O_{Earth}$ reported by Herwartz *et al*. (*21*). The yellow region encompasses the contours consistent with our data ±2 SE. Corresponding values for δ_{Theia} are shown at right. One set of δ_{Theia} values applies if the fraction of the present-day bulk silicate Earth composed of Theia is 0.1, whereas the values in parentheses apply where the fraction of Theia in present-day Earth is 0.5. For comparison, the ranges in Theia contents of the Moon and Earth for four simulated Moon-forming impact scenarios are shown as dashed horizontal lines. The models include the "canonical" model requiring no subsequent angular momentum loss by Canup (2008; Canup08), the hit-and-run model of Reufer *et al*. (2012; RMBW012), and the high angular momentum scenarios, including Cuk & Stewart (2012; C&S012) and Canup (2012; Canup012). (**B**) The cumulative probability for $\Delta'^{17}O_{Theia} - \Delta'^{17}O_{proto\text{-}Earth}$ in per mil based on simulations in this study. Three cases are shown: those with late accreted mass to Earth <5%, those with late accreted mass <1%, and all simulations.

of mass-dependent isotope fractionation. The small fractional differences in isotope ratios can be replaced with $\delta'^{17}O = 10^3\ln(^{17}R/^{17}R_o)$ and $\delta'^{18}O = 10^3\ln(^{18}R/^{18}R_o)$ (*13*) values, where ^{17}R is $^{17}O/^{16}O$, ^{18}R is $^{18}O/^{16}O$, and $^{17}R_o$ and $^{18}R_o$ refer to the initial isotope ratios (such as those characterizing bulk Earth) (*14*). These δ′ values are nearly equivalent to the fractional differences in per mil (‰) but are linearly related by the mass fractionation exponent β. The exact values for β depend on the processes involved in fractionation but are always near ½, as prescribed by oxygen isotope masses (*13*). With these definitions, $\Delta'^{17}O$ is written as

$$\Delta'^{17}O = \delta'^{17}O - \beta\delta'^{18}O \quad (1)$$

A positive $\Delta'^{17}O$ signifies that a reservoir is enriched in ^{17}O relative to Earth, whereas a negative value signifies that a reservoir is relatively depleted in ^{17}O compared with expectations from mass fractionation. At the scale of individual mineral grains, solar system materials exhibit variations in $\Delta'^{17}O$ spanning ~200‰ (*15*). The dispersion in $\Delta'^{17}O$ decreases drastically with mass. Differences in $\Delta'^{17}O$ among meteorite whole-rock samples are ~5 to 8‰ (*4*, *16*), representing parent asteroids with masses of ~10^{15} to 10^{17} kg. Differences between differentiated bodies with metal cores and silicate mantles are smaller still: Mars (6.4×10^{23} kg) has a $\Delta'^{17}O$ value of about +0.3‰, whereas Vesta (2.6×10^{20} kg) has a value of −0.25‰ (*17*, *18*). The reduced dispersion in $\Delta'^{17}O$ with mass evidently reflects averaging as smaller rocky bodies coalesced to form larger bodies in the solar system (*19*, *20*). Historically, the identical $\Delta'^{17}O$ values for Earth and the Moon have stood out against this backdrop of variability in the solar system.

However, some high-precision measurements on lunar samples indicated that the Moon has a greater $\Delta'^{17}O$ than that of Earth by 12 ± 3 parts per million (ppm) (*21*). The importance of this finding can be gauged by considering contours for $\Delta'^{17}O_{Moon} - \Delta'^{17}O_{Earth}$ plotted as functions of the difference in $\Delta'^{17}O$ between Theia and the proto-Earth and the difference in the fractions of the Moon and Earth inherited from Theia (Fig. 1A). The mass-balance equation plotted is

$$x_{Theia,Moon} - x_{Theia,Earth} = \frac{\Delta'^{17}O_{Moon} - \Delta'^{17}O_{Earth}}{\Delta'^{17}O_{Theia} - \Delta'^{17}O_{proto-Earth}} \quad (2)$$

where $x_{Theia,i}$ refers to the oxygen fraction of body *i* derived from Theia (essentially, mass fractions of the bulk silicate portions of the bodies). For convenience, we also use the fractional difference δ_{Theia} rather than the absolute difference in Eq. 2:

$$\delta_{Theia} = (x_{Theia,Moon} - x_{Theia,Earth})/x_{Theia,Earth} \quad (3)$$

The implications of a difference in oxygen isotopic composition between the Moon and Earth depend on the fraction of Theia contained within Earth (Eqs. 2 and 3). Four recent proposed giant impact scenarios (*5*, *11*, *12*, *22*) predict disparate differences in the Theia fractions in the Moon and Earth (Fig. 1A). If the difference in $\Delta'^{17}O$ between Theia and the proto-Earth was zero, there is no oxygen isotope constraint on δ_{Theia} (Fig. 1A). Similarly, if Earth and the Moon are composed of precisely the same concentrations of Theia, there is no constraint on differences in $\Delta'^{17}O$ between Theia and the proto-Earth.

A positive $\Delta'^{17}O$ of 12 ± 3 ppm for the Moon (*21*) requires a difference in the proportions of Moon and Earth composed of remnants of Theia because the contours representing this range of values (Fig. 1A, pink regions) do not include the center of the diagram (Fig. 1A). For a Mars-sized differentiated body with $\Delta'^{17}O$ ~ ± 0.3‰ (such as Mars or Vesta), the difference in Theia contents between the Moon and Earth is ± 50% or more (Fig. 1A). For the case of a proto-Earth–sized Theia, the result is a difference of ± 8% or more (Fig. 1A). Alternatively, assuming enstatite-chondrite–like material better represents the terrestrial planet-forming region (*23*, *24*), differences in oxygen isotope ratios between Theia and proto-Earth would have been smaller (~0.1‰) (*21*, *25*), and the lunar $\Delta'^{17}O$ of 12 ± 3 ppm (*21*) requires δ_{Theia} values of 150 and 30% for the Mars and proto-Earth–sized impactors, respectively (Fig. 1A). Such large δ_{Theia} values would effectively remove the constraint imposed by oxygen isotopes that the Earth-Moon system was well mixed.

We analyzed seven Apollo 12, 15, and 17 lunar samples and one lunar meteorite and compared their $^{17}O/^{16}O$ and $^{18}O/^{16}O$ isotope ratios with those for a suite of terrestrial igneous samples. The 1- to 4-mg lunar samples include high-Ti mare basalts, low-Ti Mg-rich olivine cumulate basalts, a quartz normative basalt, and a highland

Table 1. Summary of oxygen isotope data for lunar and terrestrial samples. Delta values are in logarithmic form as defined in the text.

Sample	$\delta'^{17}O$	$\delta'^{18}O$	$\Delta'^{17}O$
Lunar basalt			
Average (*n* = 8)	3.004	5.691	−0.001
Standard deviation	0.090	0.172	0.005
Standard error	0.032	0.061	0.002
Lunar basalt-fused beads			
Average (*n* = 4)	2.940	5.572	0.000
Standard deviation	0.133	0.245	0.006
Standard error	0.067	0.123	0.003
Lunar troctolite			
Average (*n* = 2)	3.178	6.050	−0.016
Standard deviation	0.009	0.026	0.005
Standard error	0.007	0.019	0.003
San Carlos olivine			
Average (*n* = 17)	2.711	5.134	0.000
Standard deviation	0.072	0.134	0.005
Standard error	0.017	0.033	0.001
Mauna Loa olivine			
Average (*n* = 4)	2.736	5.189	−0.004
Standard deviation	0.090	0.170	0.001
Standard error	0.045	0.085	0.001
Mauna Loa whole-rock samples			
Average (*n* = 5)	2.796	5.298	−0.002
Standard deviation	0.031	0.063	0.003
Standard error	0.014	0.028	0.001
San Carlos spinel			
Average (*n* = 2)	2.171	4.104	0.004
Standard deviation	0.135	0.285	0.015
Standard error	0.096	0.202	0.011
Bushveld anorthosite			
Average (*n* = 2)	3.522	6.694	−0.012
Standard deviation	0.002	0.002	0.001
Standard error	0.001	0.002	0.000
Gore Mountain garnet			
Average (*n* = 2)	3.174	6.020	−0.004
Standard deviation	0.017	0.026	0.003
Standard error	0.012	0.019	0.002

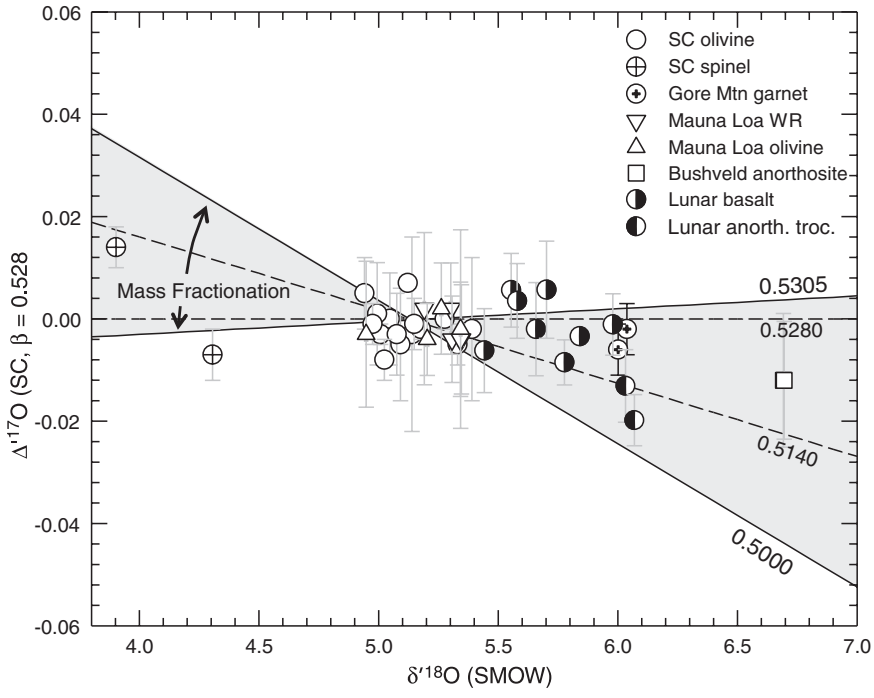

Fig. 2. Plot of $\Delta'^{17}O$ versus $\delta'^{18}O$ for lunar and terrestrial samples by using a fractionation line with β = 0.528 passing through San Carlos olivine as the reference. Only the powders of lunar samples are plotted. The gray region indicates the regions accessible through mass fractionation starting from SC olivine. Different fractionation laws are labeled with their defining β values. Error bars depict 2 SE for each measurement. Points lying inside of the gray region are consistent with simple one-stage, mass-dependent isotope fractionation relative to SC olivine, implying that they represent a single oxygen reservoir.

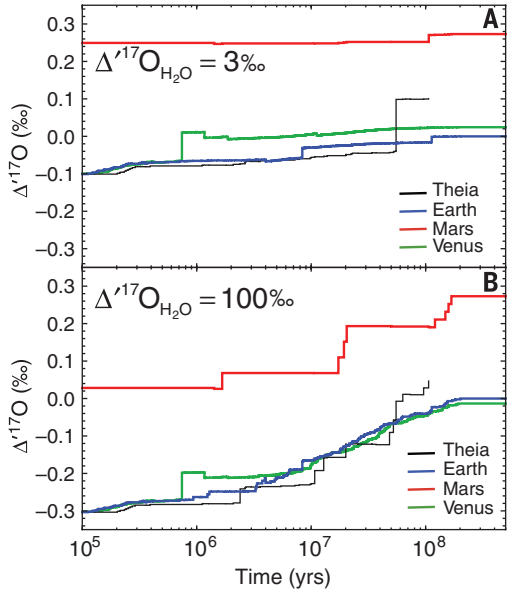

Fig. 3. A simulation of the oxygen isotopic evolution of the terrestrial planets and last giant (Moon-forming) impactor, Theia. The $\Delta'^{17}O$ values of the growing Venus-like (green), Earth-like (blue), and Mars-like (red) planets are shown as a function of time as well as the value for the Theia-like impactor (black). (**A**) The case in which the water oxygen reservoir has $\Delta'^{17}O$ = 3‰. (**B**) The case in which water $\Delta'^{17}O$ = 100‰.

anorthositic troctolite (table S1). The terrestrial samples include San Carlos mantle xenolith olivines, San Carlos mantle xenolith spinels, Mauna Loa basalt samples, Mauna Loa olivine separates, an anorthosite from the Bushveld complex, and a sample of Gore Mountain metamorphic garnet. We obtained our analyses (Table 1) using infrared laser heating (*26*) modified to include F_2 as the fluorinating agent and purification of the analyte O_2 gas for analysis of both $^{17}O/^{16}O$ and $^{18}O/^{16}O$ (*27*). We have improved our precision compared with many previous efforts by more thoroughly desiccating samples before analysis and by regular rebalancing of standard and sample ion beam intensities throughout the mass spectrometer analyses (*28*). We analyzed a range of lunar and terrestrial sample lithologies to account for the fact that β values vary with process (*13*, *29*, *30*). We use the traditional standard mean ocean water (SMOW) as the reference for $\delta'^{18}O$, but we use San Carlos (SC) olivine as the reference for $\Delta'^{17}O$ when characterizing oxygen isotope reservoirs of rocks (*28*). We adopt a typical igneous β of 0.528 passing through the mean value for San Carlos olivine as our reference fractionation line for calculating $\Delta'^{17}O$ (*28*).

Lunar basalts are relatively high in $\delta'^{18}O$ as compared with SC olivine and terrestrial basalts (Fig. 2). Nonetheless, the basalts show no clear deviation from the reference β of 0.528, allowing direct comparison of $\Delta'^{17}O$ values for these materials. No discernible difference exists in $\Delta'^{17}O$ between SC olivine and lunar basalts powders (−0.001 ± 0.002, 1 SE) or fused beads (0.000 ± 0.003, 1 SE). The mean for all mafic terrestrial samples, representing terrestrial mantle and its melt products, is 0.000 ± 0.001‰ (1 SE). Adding in quadrature, the analytical uncertainty in the SC olivine and the standard error for the lunar samples yields a difference between lunar basalt and SC olivine of −0.001 ± 0.0048‰ (−1 ± 4.8 ppm, 2 SE), which is indistinguishable from zero. Other mafic terrestrial whole rocks and olivines are within this uncertainty range (Table 1). We found no resolvable difference in $\Delta'^{17}O$ between lunar mantle melts represented by these basalts and terrestrial mantle and melts.

Our result does not agree with the conclusions of Herwartz *et al.* (*21*). Measurements on the one sample common to both studies (12018) agree within uncertainties when compared in the same reference frame (fig. S2) (*28*). It is therefore conceivable that an unfortunate difference in sample selection could be a plausible explanation for the difference between the studies.

The lunar highland sample has a significantly lower $\Delta'^{17}O$ value of −0.016 ± 0.003‰ (1 SE) (or −16 ± 3 ppm), which is similar to a previous study (*8*). However, the terrestrial anorthosite sample has a similarly low value (Table 1). The low $\Delta'^{17}O$ values for both the terrestrial and lunar highland anorthosites (anorthostic troctolite) imply a mass fractionation process related to formation of this rock type that results in low $\Delta'^{17}O$ values (Fig. 2). The low $\Delta'^{17}O$ value for the lunar highland rocks is not evidence for a distinction between the oxygen pools for the Moon and Earth because these samples are in the mass-fractionation envelope for Earth (Fig. 2), and low $\Delta'^{17}O$ values are found

in both terrestrial and lunar anorthosite-like rocks. One terrestrial mantle spinel sample also shows a measurable deviation from the $\beta = 0.528$ reference, implying a relatively low β value (Fig. 2).

Of course, in all cases invoking no difference in oxygen isotope ratios between Theia and proto-Earth results in no constraints on the relative Theia concentrations in the Moon and Earth. We can assess the purely statistical feasibility of two proto-planetary bodies having identical oxygen isotope ratios using the central limit theorem (*19*). Results suggest that a purely random sampling of asteroid-like materials would lead to variations in $\Delta'^{17}O$ among planetary embryos of ~3 ppm (*28*). However, the larger difference between Earth and Mars testifies to the fact that $\Delta'^{17}O$ was not distributed randomly in small bodies across the inner solar system.

Differences in $\Delta'^{17}O$ between Theia and the proto-Earth have expected values of 0.15‰ (*31*) or 0.05 ‰ (*32*) on the basis of two recent N-body simulations of standard terrestrial planet-formation scenarios with hypothesized gradients in $\Delta'^{17}O$ across the inner solar system. We used a planetary accretion model (*33*) that uses N-body accretion simulations based on the Grand Tack scenario (*34*). Our model differs from previous efforts in that we strictly limit our analysis to simulations that closely reproduce the current masses and locations of Earth and Mars and the oxidation state of Earth's mantle, we use a multi-reservoir model (composed of silicate, oxidized iron, and water) to describe the initial heliocentric distribution of oxygen isotopes, and we include the effects of mass accretion subsequent to the Moon-forming impact (*28*). An example simulation (Fig. 3) and others like it show that the $\Delta'^{17}O$ values of the colliding bodies rise together as the average $\Delta'^{17}O$ values increase during accretion. Incorporation of more material from greater distances from the Sun as accretion proceeds accounts for the rise. Large planets such as Earth and Venus reflect an average of many embryos and planetesimals and so exhibit similar $\Delta'^{17}O$ values with time, whereas stranded embryos averaging fewer components, such as Mars, show greater variation.

The cumulative distribution of $\Delta'^{17}O$ differences between Theia and proto-Earth is shown for 236 simulations of planet growth (*35*) (Fig. 1B). The median $\Delta'^{17}O_{Theia} - \Delta'^{17}O_{proto\text{-}Earth}$ is nearly 0 in these calculations for all simulations (Fig. 1B). However, our median predicted $\Delta'^{17}O_{Theia} - \Delta'^{17}O_{proto\text{-}Earth}$ is +0.1‰ if we restrict our analysis to those simulations consistent with adding ≤1% by mass of a "late veneer" (LV) of primitive material post Moon-forming giant impact, as required by geochemical constraints (*36*). This median value combined with our measurement of $\Delta'^{17}O_{Moon} - \Delta'^{17}O_{Earth}$ corresponds to δ_{Theia} of +20 to −60% for the Mars-sized impactor scenario and +8 to −12% in the proto-Earth–sized impactor scenarios. The corresponding values for δ_{Theia} using the previous 12 ± 3 ppm difference between Moon and Earth $\Delta'^{17}O$ values (*21*) are +80 to +180% and +16 to +36%, respectively (Fig. 1A). The new measurements presented here are consistent with Earth and the Moon having near-identical Theia contents. Indistinguishable $\Delta'^{17}O$ values of the Moon and Earth to the 5 ppm level of uncertainty suggests that the Moon-forming impact thoroughly mixed and homogenized the oxygen isotopes of Theia and proto-Earth.

Our interpretation has implications for the composition of the LV of primitive bodies that impacted the silicate Earth. A disproportionately larger flux of LV planetesimals is implied by a higher average $^{182}W/^{184}W$ for the Moon than for Earth and by previous estimates for the apparent differences in highly siderophile element (HSE) concentrations between the terrestrial and lunar mantles (*37*). The interpretation of these data is that the Moon and Earth began with the same W isotopic ratios, but that Earth inherited a greater fraction of low $^{182}W/^{184}W$ material in the form of chondritic planetesimals after the Moon-forming giant impact (*38*, *39*). If we adopt the conclusion from the W isotopes that the Earth-Moon system was well mixed as a result of the Moon-forming impact, then the nearly identical $\Delta'^{17}O$ values of Moon and Earth constrain the identity of the LV impactors by their oxygen isotope ratios. Estimates for the Earth/Moon ratio of the LV mass fluxes range from ~200 to 1200 (*37*, *40*, *41*). Using a late-veneer flux to Earth of 2×10^{22} kg (*37*) and a conservative maximum Earth/Moon flux ratio of 1200 (*41*), the difference in LV fractions comprising the silicate Earth and Moon is 0.00447. Combining this value with our measured value for $\Delta'^{17}O_{Moon} - \Delta'^{17}O_{Earth}$ of zero (28) requires that the LV impactors had average $\Delta'^{17}O$ values within ~0.2‰ or less of Earth, similar to enstatite chondrites (*25*). Alternatively, with our maximum permitted $\Delta'^{17}O_{Moon} - \Delta'^{17}O_{Earth}$ of ± ~5 ppm, the calculated $\Delta'^{17}O$ value for the LV is ±1.1‰. This value encompasses aqueously altered carbonaceous chondrites and some ordinary chondrites. For comparison, the same calculation using the 12 ppm difference between the Moon and Earth yields an LV $\Delta'^{17}O$ of −2.7‰, suggesting that the impactors were composed mainly of relatively unaltered and dry carbonaceous chondrites (*4*). Our result suggests that if the LV was composed mainly of carbonaceous chondrites, the parent bodies must have included substantial fractions of high-$\Delta'^{17}O$ water either in the form of aqueous alteration minerals or as water ice.

REFERENCES AND NOTES

1. W. K. Hartmann, D. R. Davis, *Icarus* **24**, 504–515 (1975).
2. S. A. Jacobson *et al.*, *Nature* **508**, 84–87 (2014).
3. R. N. Clayton, *Annu. Rev. Earth Planet. Sci.* **21**, 115–149 (1993).
4. R. N. Clayton, N. Onuma, T. K. Mayeda, *Earth Planet. Sci. Lett.* **30**, 10–18 (1976).
5. R. M. Canup, *Icarus* **196**, 518–538 (2008).
6. K. Pahlevan, D. J. Stevenson, *Earth Planet. Sci. Lett.* **262**, 438–449 (2005).
7. R. M. Canup, E. Asphaug, *Nature* **412**, 708–712 (2001).
8. U. Wiechert *et al.*, *Science* **294**, 345–348 (2001).
9. L. J. Hallis *et al.*, *Geochim. Cosmochim. Acta* **74**, 6885–6899 (2010).
10. M. J. Spicuzza, J. M. D. Day, L. A. Taylor, J. W. Valley, *Earth Planet. Sci. Lett.* **253**, 254–265 (2007).
11. R. M. Canup, *Science* **338**, 1052–1055 (2012).
12. M. Ćuk, S. T. Stewart, *Science* **338**, 1047–1052 (2012).
13. E. D. Young, A. Galy, H. Nagahara, *Geochim. Cosmochim. Acta* **66**, 1095–1104 (2002).
14. C. R. McKinney, J. M. McCrea, S. Epstein, H. A. Allen, H. C. Urey, *Rev. Sci. Instrum.* **21**, 724–730 (1950).
15. N. Sakamoto *et al.*, *Science* **317**, 231–233 (2007).
16. M. K. Weisberg *et al.*, *Geochim. Cosmochim. Acta* **55**, 2657–2669 (1991).
17. I. A. Franchi, I. P. Wright, A. S. Sexton, C. T. Pillinger, *Meteorit. Planet. Sci.* **34**, 657–661 (1999).
18. R. N. Clayton, T. K. Mayeda, *Geochim. Cosmochim. Acta* **60**, 1999–2017 (1996).
19. J. A. Nuth III, H. G. M. Hill, *Meteorit. Planet. Sci.* **39**, 1957–1965 (2004).
20. V. S. Safronov, *Sov. Astron.* **9**, 987–991 (1966).
21. D. Herwartz, A. Pack, B. Friedrichs, A. Bischoff, *Science* **344**, 1146–1150 (2014).
22. A. Reufer, M. M. M. Meier, W. Benz, R. Wieler, *Icarus* **221**, 296–299 (2012).
23. S. B. Jacobsen, M. I. Petaev, S. Huang, paper presented at the American Geophysical Union Fall Meeting, San Francisco, CA, 2012.
24. L. R. Nittler *et al.*, *Science* **333**, 1847–1850 (2011).
25. J. Newton, I. A. Franchi, C. T. Pillinger, *Meteorit. Planet. Sci.* **35**, 689–698 (2000).
26. Z. D. Sharp, *Geochim. Cosmochim. Acta* **54**, 1353–1357 (1990).
27. E. D. Young, H. Nagahara, B. O. Mysen, D. M. Audet, *Geochim. Cosmochim. Acta* **62**, 3109–3116 (1998).
28. Materials and methods are available as supplementary materials on *Science* Online.
29. X. Cao, Y. Liu, *Geochim. Cosmochim. Acta* **75**, 7435–7445 (2011).
30. J. Matsuhisa, J. R. Goldsmith, R. N. Clayton, *Geochim. Cosmochim. Acta* **42**, 173–182 (1978).
31. N. A. Kaib, N. B. Cowan, *Icarus* **252**, 161–174 (2015).
32. A. Mastrobuono-Battisti, H. B. Perets, S. N. Raymond, *Nature* **520**, 212–215 (2015).
33. D. C. Rubie *et al.*, *Icarus* **248**, 89–108 (2015).
34. K. J. Walsh, A. Morbidelli, S. N. Raymond, D. P. O'Brien, A. M. Mandell, *Nature* **475**, 206–209 (2011).
35. S. A. Jacobson, A. Morbidelli, *Philos. Trans. A Math. Phys. Eng. Sci.* **372**, 20130174 (2014).
36. C.-L. Chou, *Proc. Lunar. Planet. Sci. Conf.* **9**, 219–230 (1978).
37. R. J. Walker *et al.*, *Chem. Geol.* **411**, 125–142 (2015).
38. T. S. Kruijer, T. Kleine, M. Fischer-Gödde, P. Sprung, *Nature* **520**, 534–537 (2015).
39. M. Touboul, I. S. Puchtel, R. J. Walker, *Nature* **520**, 530–533 (2015).
40. H. E. Schlichting, P. H. Warren, Q.-Z. Yin, *Astrophys. J.* **752**, 8 (2012).
41. W. F. Bottke, R. J. Walker, J. M. D. Day, D. Nesvorny, L. Elkins-Tanton, *Science* **330**, 1527–1530 (2010).

ACKNOWLEDGMENTS

We are grateful to NASA Johnson Space Center for approving use of the Apollo samples for this study. E.D.Y. acknowledges support from a grant from the NASA Emerging Worlds program (NNX15AH43G). D.C.R., S.A.J., and A.M. acknowledge support from the European Research Council Advanced Grant "ACCRETE" (contract 290568). Development of the Panorama instrument was supported by the Deep Carbon Observatory (Sloan Foundation), NSF, U.S. Department of Energy, Shell, the Carnegie Institution of Washington, and the University of California, Los Angeles. The complete data table for this study can be found in the supplementary materials.

SUPPLEMENTARY MATERIALS

www.sciencemag.org/content/351/6272/493/suppl/DC1
Materials and Methods
SupplementaryText
Figs. S1 to S7
Tables S1 to S4
References (*42*–*67*)

18 July 2015; accepted 13 December 2015
10.1126/science.aad0525

Oxygen isotopic evidence for vigorous mixing during the Moon-forming giant impact

Edward D. Young, Issaku E. Kohl, Paul H. Warren, David C. Rubie, Seth A. Jacobson and Alessandro Morbidelli

Science **351** (6272), 493-496.
DOI: 10.1126/science.aad0525

Rehomogenizing the Earth-Moon system

A giant impact formed the Moon, and lunar rocks provide insight into that process. Young *et al.* found that rocks on Earth and the Moon have identical oxygen isotopes. This suggests that well-mixed material from the giant impact must have formed both the Moon and Earth's mantle. The finding also constrains the composition of the "late veneer": material sprinkled onto Earth after the Moon-forming impact.

Science, this issue p. 493